20. P. A. Underhill *et al.*, *Ann. Hum. Genet.* **65**, 43 (2001).
21. P. A. Underhill *et al.*, *Nature Genet.* **26**, 358 (2000).
22. A. W. Bergen *et al.*, *Ann. Hum. Genet.* **63**, 63 (1999).
23. M. H. Wolpoff, J. Hawks, R. Caspari, *Am. J. Phys. Anthropol.* **112**, 129 (2000).
24. L. Jin, B. Su, *Nature Rev. Genet.* **1**, 126 (2000).
25. M. Stoneking *et al.*, *Curr. Opin. Genet. Dev.* **6**, 731 (1996).
26. R. M. Harding *et al.*, *Am. J. Hum. Genet.* **60**, 772 (1997).
27. H. Kaessmann, F. Heissig, A. Haeseler, S. Paabo, *Nature Genet.* **22**, 78 (1999).
28. E. Harris, J. Hey, *Proc. Natl. Acad. Sci. U.S.A.* **96**, 3320 (1999).
29. Z. M. Zhao *et al.*, *Proc. Natl. Acad. Sci. U.S.A.* **97**, 11354 (2000).
30. J. C. Fay, C. I. Wu, *Mol. Biol. Evol.* **16**, 1003 (1999).

31. We thank all the 12,127 men who donated DNA for this study. This study was supported by the China Natural Science Foundation. B.S., R.C., and L.J. were supported by NIH grants. R.D. was supported by the Center for Environmental Genetics at the University of Cincinnati.

20 February 2001; accepted 20 March 2001

Spermiogenesis Deficiency in Mice Lacking the *Trf2* Gene

Di Zhang,[1] Tarja-Leena Penttila,[3] Patricia L. Morris,[2,3] Martin Teichmann,[1] Robert G. Roeder[1]*

The discovery of TATA-binding protein–related factors (TRFs) has suggested alternative mechanisms for gene-specific transcriptional regulation and raised interest in their biological functions. In contrast to recent observations of an embryonic lethal phenotype for TRF2 inactivation in *Caenorhabditis elegans* and *Xenopus laevis*, we found that *Trf2*-deficient mice are viable. However, *Trf2*$^{-/-}$ mice are sterile because of a severe defect in spermiogenesis. Postmeiotic round spermatids advance at most to step 7 of differentiation but fail to progress to the elongated form, and gene-specific transcription deficiencies were identified. We speculate that mammals may have evolved more specialized TRF2 functions in the testis that involve transcriptional regulation of genes essential for spermiogenesis.

Early studies have suggested that one universal TATA-binding protein (TBP) functions as a central component of the general transcription machineries to mediate transcription by nuclear RNA polymerases I, II, and III in eukaryotes (*1*). However, the identification of two TBP-related factors (TRF1 and TRF2) raised the possibility that TRFs may substitute for TBP in mediating the transcription of specific genes and thus have distinct biological functions (*2–5*). In *Drosophila*, biochemical studies have documented promoter-specific functions of TRF1 (*6, 7*). In both *Caenorhabditis elegans* and *Xenopus laevis*, inactivation of TRF2 results in embryonic lethality and deficiencies in embryonic gene transcription (*8–10*). However, except for the observation that TRF2 is abundantly expressed in the testis of human and mouse (*4, 5*), there has been no information regarding biological functions of TRF2 in mammalian species.

To elucidate the functional role of TRF2, we used homologous recombination in embryonic stem cells to generate mice lacking a functional *Trf2* gene (*11*). We constructed a targeting vector in which a region containing the central four exons of *Trf2* was replaced by a neomycin resistance gene cassette (*11*). This deletion eliminates nearly 80% of the core region of TRF2. Genotyping of 218 F_2 offspring by polymerase chain reaction analysis revealed a *Trf2*$^{+/+}$:*Trf2*$^{+/-}$:*Trf2*$^{-/-}$ distribution (69:109:40) that does not deviate significantly from the expected Mendelian ratio, although there could be some earlier lethality of homozygous embryos. Disruption of the *Trf2* gene was confirmed by Southern blot analysis (*11*). Subsequent Northern blot analyses of testis RNAs from *Trf2* mutant mice showed reduced expression of full-length *Trf2* transcripts in heterozygotes and no expression in homozygotes (*11*).

Mice deficient for the *Trf2* gene appeared to be healthy and showed no apparent abnormalities in major organs at the gross and histological levels. However, testes from the adult *Trf2*-deficient mice showed size and weight reductions of ~50% in comparison with those from the wild-type and heterozygous controls (*11*). When *Trf2*$^{-/-}$ male mice were mated with *Trf2*$^{+/+}$ female mice, they copulated normally, as evidenced by the formation of vaginal plugs in their mates, but none of the mated female mice became pregnant. In contrast, *Trf2*$^{-/-}$ females were fertile and produced normal average litter sizes (7.3 ± 1.8; n = 10). Analyses of serum testosterone levels in *Trf2*$^{-/-}$ male mice revealed no statistically significant difference in comparison to their *Trf2*$^{+/+}$ or *Trf2*$^{+/-}$ littermates (*11*). We next evaluated semen samples extracted from the vas deferens and epididymis. The seminal fluid from *Trf2*$^{-/-}$ mice lacked spermatozoa, whereas there were no apparent differences in sperm number or morphology between *Trf2*$^{+/+}$ and *Trf2*$^{+/-}$ mice (*11*).

In the testis, male germ cells differentiate from spermatogonia into spermatozoa by a complex process referred to as "spermatogenesis." The mouse spermatogenesis cycle is well defined and can be subdivided into 12 stages, with each stage consisting of a specific complement of male germ cells. In determining the nature of the sperm deficiency, we analyzed male germ cell differentiation both in adult mice and in juvenile mice between 8 and 35 days after birth. In the latter case, the first wave of developing germ cells progresses through spermatogenesis with specific mitotic and meiotic cells first appearing according to a well-characterized developmental program (*12*). Inspection of seminiferous tubules in the adult

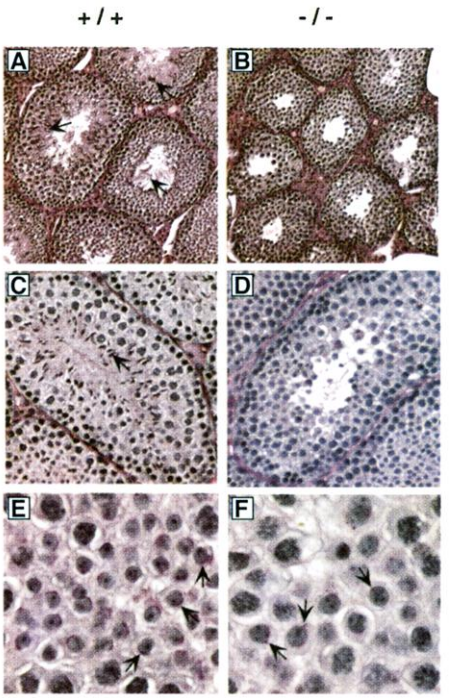

Fig. 1. *Trf2*$^{-/-}$ mice show defects in spermiogenesis. (**A** and **B**) Histological analysis of testis sections from adult *Trf2*$^{+/+}$ (A) and *Trf2*$^{-/-}$ (B) littermates. Magnification, ×200. Arrows indicate the elongated spermatids or spermatozoa that are present in *Trf2*$^{+/+}$ but absent in the *Trf2*$^{-/-}$ testis. (**C** and **D**) Histological analysis of testis sections from *Trf2*$^{+/+}$ (C) and *Trf2*$^{-/-}$ (D) juvenile mice of 28 days of age. Magnification, ×200. The arrow indicates the elongated spermatids that are present in *Trf2*$^{+/+}$ but absent in the *Trf2*$^{-/-}$ testis. (**E** and **F**) Morphology of seminiferous tubules at stage VI from *Trf2*$^{+/+}$ (E) and *Trf2*$^{-/-}$ (F) juvenile mice of 25 days of age. Magnification, ×1000. Arrows indicate the acrosomes of the spermatids, which are stained pink. The acrosomal structures are abnormal in the *Trf2*$^{-/-}$ section, as compared to the *Trf2*$^{+/+}$ section.

[1]Laboratory of Biochemistry and Molecular Biology, [2]The Rockefeller University, New York, NY 10021, USA. [3]Population Council, New York, NY 10021, USA.

*To whom correspondence should be addressed. E-mail: roeder@rockvax.rockefeller.edu

testis revealed a 20 to 30% reduction in diameter in those from *Trf2*$^{-/-}$ mice (Fig. 1B) as compared to those from *Trf2*$^{+/+}$ mice (Fig. 1A). Further analyses indicated that although somatic Sertoli and Leydig cells, spermatogonia, and spermatocytes appeared to be normal, and whereas both spermatogonial mitoses and spermatocyte meioses were commonly observed, the postmeiotic cells were abnormal in the tubules of *Trf2*$^{-/-}$ mice. Thus, both adult mice (Fig. 1B) and 28-day (Fig. 1D) or older juvenile mice showed a complete absence of elongated spermatids or spermatozoa and the presence of large visible vacuolar structures inside the tubules of mutant testes, whereas elongated spermatids developed in the wild-type testes (Fig. 1, A and C). Furthermore, both in adult mice and in juvenile mice (Fig. 1F) between 22 and 26 days of age, round spermatid development was interrupted at different steps during spermiogenesis, as judged by the abnormal appearance of acrosome structures, as compared to those in the wild-type counterpart (Fig. 1E). Some spermatids proceeded until step 7 but failed to undergo morphological differentiation and development into elongated spermatids in *Trf2*$^{-/-}$ mice. Therefore, we conclude that the *Trf2*-deficient mice have a severe defect in spermiogenesis (the process by which spermatids morphologically and structurally transform into mature spermatozoa).

In the *Trf2*$^{-/-}$ mice, we observed that some cells in stage VIII to stage X tubules had degenerated, with abnormal nuclear structures and increased chromosomal density (Fig. 2B, arrowheads) in comparison with those of *Trf2*$^{+/+}$ mice (Fig. 2A). We also observed multinucleated giant cells (Fig. 2B, arrows), which previously have been shown to correspond to apoptotic germ cells (*13*), in these tubules. A TUNEL (for terminal deoxytransferase–mediated deoxyuridine triphosphate– biotin nick end labeling) assay revealed large numbers of apoptotic cells in some tubules in *Trf2*$^{-/-}$ testes (Fig. 2D). Such cells were rare in sections from the *Trf2*$^{+/+}$ testes and were mainly located next to the basal lamina of the tubules (Fig. 2C) (*11*). The occurrence of apoptotic cells in the testes of juvenile mice was also investigated. Whereas the relative proportion of sporadic apoptotic cells decreases overall as wild-type testes mature from day 22 to day 32 of age (Fig. 2E), apoptotic cells become more prevalent in the juvenile testis of *Trf2*-deficient mice at day 28 after birth and beyond (Fig. 2F). Together, these data indicate that the absence of TRF2 results both in a failure of spermatid differentiation and an increase in apoptosis.

We think that the spermatogenesis defect in *Trf2*$^{-/-}$ mice is intrinsic to the germ cells because our previous in situ hybridization and Northern blot analyses revealed that high-level TRF2 expression in the testis is confined exclusively to male germ cells in a stage-specific manner (*5, 14*). TRF2 expression was first detected in late pachytene spermatocytes at stage VIII and increased throughout subsequent stages. After meiotic divisions, TRF2 expression declined continuously in the round spermatids during progression from stage I to stage V. This indicates that TRF2 might be critical for spermiogenesis through the appropriate regulation of genes acting in spermatid differentiation.

To investigate the effect of *Trf2* deficiency on potential downstream targets, testis RNAs from adult *Trf2*$^{+/+}$ and *Trf2*$^{-/-}$ mice were analyzed with a panel of testis-specific genes (Fig. 3A) (*11*). Several genes that begin to be transcribed before the first meiotic division, such as the acrosomal serine protease *Proacrosin* (*15*), the heat-shock protein *Hsp70-2* (*16*), and histone *H1t* (*17*), showed only slightly reduced expression in the *Trf2*$^{-/-}$ mice (Fig. 3A). In contrast, postmeiotically expressed genes, such as the heat-shock protein gene *Hsc70t* (*18*), the mitochondrial capsule selenoprotein gene *Mcs* (*19*), the glyceraldehyde 3-phosphate dehydrogenase gene *Gapd-s* (*20*), and the sperm fibrous sheath component gene *Fsc-1* (*21*), showed severalfold reduced expression levels in *Trf2*$^{-/-}$ testes (Fig. 3A). The mRNA expression levels of transition proteins 1 and 2 (Tp 1 and Tp 2) and protamines 1 and 2 were dramatically reduced in *Trf2*$^{-/-}$ mice (Fig. 3A). Transition proteins and protamines are small, highly basic proteins that facilitate compaction of the mammalian sperm head during spermiogenesis (*22*), and *Tp 1*–deficient mice exhibit abnormal spermatogenesis and reduced fertility (*23*).

The reduced expression of the postmeiotic genes in the adult testis could reflect a TRF2-dependent transcriptional defect and/or the lack of elongated spermatids in *Trf2*$^{-/-}$ testes. To distinguish between these two possibilities, we also analyzed gene expression during juvenile testis development (Fig. 3B). We observed a substantial reduction in the expression of *Tp 1*, *Protamine 1*, and *Hsc70t* in the *Trf2*$^{-/-}$ mice at

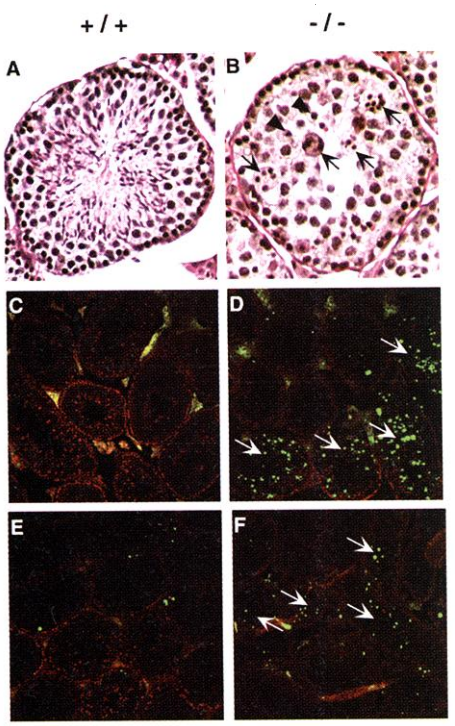

Fig. 2. Round spermatids in the testes of *Trf2*$^{-/-}$ mice undergo apoptosis. (**A** and **B**) Morphology of seminiferous tubules at stage IX from the *Trf2*$^{+/+}$ (A) and *Trf2*$^{-/-}$ (B) adult mice. Magnification, ×400. Arrows and arrowheads in (B) indicate the characteristic multinucleated giant cells and cells with abnormal nuclear structure, respectively. (**C** through **F**) In situ labeling of apoptotic cells in sections of the seminiferous tubules from *Trf2*$^{+/+}$ (C and E) and *Trf2*$^{-/-}$ (D and F) animals with the TUNEL assay. Adult animals (C and D) or juvenile animals 28 days of age (E and F) are shown. All nuclei were counterstained red with propidium iodide. Arrows in (D and F) indicate the tubules in which the apoptotic cells were stained green-yellow. The staining of cells in the interstitial areas is nonspecific.

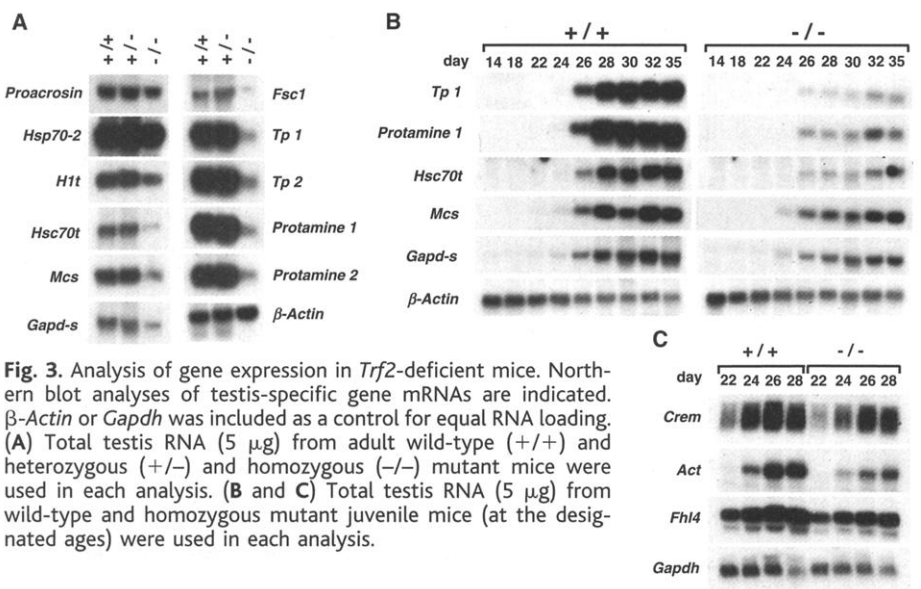

Fig. 3. Analysis of gene expression in *Trf2*-deficient mice. Northern blot analyses of testis-specific gene mRNAs are indicated. β-*Actin* or *Gapdh* was included as a control for equal RNA loading. (**A**) Total testis RNA (5 μg) from adult wild-type (+/+) and heterozygous (+/–) and homozygous (–/–) mutant mice were used in each analysis. (**B** and **C**) Total testis RNA (5 μg) from wild-type and homozygous mutant juvenile mice (at the designated ages) were used in each analysis.

26 days of age, when the most advanced differentiated cells are round spermatids (Fig. 3B). This early reduction cannot be explained by the lack of elongated spermatids in *Trf2*$^{-/-}$ testes, because in normal *Trf2*$^{+/+}$ testes these cells do not appear until 28 days of age (Fig. 1C). In contrast, the *Mcs* and *Gapd-s* genes were expressed at comparable levels in *Trf2*$^{-/-}$ and wild-type testes at 26 days of age (Fig. 3B), indicating gene-selective effects of TRF2 at this stage. Although the *Mcs* and *Gapd-s* genes did show reduced expression after 28 days of age, this likely reflects the absence of elongated spermatids at these later stages, and the overall reduction was still far less severe than that observed for the *Tp 1*, *Protamine 1*, and *Hsc70t* genes. These data from the juvenile testis analyses suggest that even though many genes are actively transcribed during the early phase of spermatid differentiation (*24*), TRF2 may not have a general role in the augmentation of overall levels of polymerase II transcription. Instead, it might regulate the differentiation program for spermiogenesis through its ability to selectively activate specific downstream target genes in round spermatids.

We noted that mice lacking the transcriptional activator CREM (cyclic AMP–responsive element modulator) also show a disruption in spermiogenesis (*13, 25*). However, our *Trf2*$^{-/-}$ mice exhibit a developmental block at a later step of spermatid differentiation, as judged from histological and marker gene expression analyses. In addition, an analysis during juvenile testis development revealed no significant differences between *Trf2*$^{-/-}$ and *Trf2*$^{+/+}$ testes in the expression of CREM (*26*) and the testis-specific CREM coactivator FHL4 (*27*), especially when normalized to *Gapdh* expression (Fig. 3C). Moreover, TRF2 deficiency had only a moderate effect on expression of the CREM coactivator ACT (*28*) (Fig. 3C).

Through targeted inactivation, we demonstrated the importance of TRF2 in the normal differentiation program of mouse spermiogenesis. The specific effects of the *Trf2* mutation on spermiogenesis indicate that *Trf2*$^{-/-}$ mice could be valuable for the study of some types of idiopathic infertility in men (*29*). Our study reveals that the physiological consequences of *Trf2* deficiency in mouse differ from those of TRF2 deficiencies in *C. elegans* and *Xenopus* (*8–10*). The normal embryonic development of *Trf2*$^{-/-}$ mice is most likely not a result of a maternal contribution of normal TRF2 protein, because *Trf2*$^{-/-}$ females are fertile. On the other hand, the embryonic lethal phenotypes in *C. elegans* and *Xenopus* have prevented further analyses of the possibility that TRF2 has an additional role(s) in male germ cell differentiation in these organisms. The functions of TRF2 might reflect differences in TRF2 expression patterns in these organisms (*5, 8–10*) or differences in TRF2 protein sequences, even though these proteins appear homologous among different species (*2*). Particularly, we note that mouse TRF2 is composed mainly of a core region of 180 amino acids, with a very short NH_2-terminal region, whereas the *C. elegans* TRF2 has a much longer NH_2-terminal sequence, an additional COOH-terminal sequence, and an insertion of ~100 amino acids in the core region (*2*). Another possibility is that the biological functions mediated by TBP and TRF2 may be distinct in different species. We propose that TBP or another protein may have taken over the role of TRF2 in mouse embryonic development and that TRF2 functions may have become restricted to specialized functions in the testis.

References and Notes

1. S. K. Burley, R. G. Roeder, *Annu. Rev. Biochem.* **65**, 769 (1996).
2. J. C. Dantonel, J. M. Wurtz, O. Poch, D. Moras, L. Tora, *Trends Biochem. Sci.* **24**, 335 (1999).
3. S. K. Hansen, S. Takada, R. H. Jacobson, J. T. Lis, R. Tjian, *Cell* **91**, 71 (1997).
4. T. Ohbayashi, Y. Makino, T. Tamura, *Nucleic Acids Res.* **27**, 750 (1999).
5. M. Teichmann *et al.*, *Proc. Natl. Acad. Sci. U.S.A.* **96**, 13720 (1999).
6. S. Takada, J. T. Lis, S. Zhou, R. Tjian, *Cell* **101**, 459 (2000).
7. M. C. Holmes, R. Tjian, *Science* **288**, 867 (2000).
8. L. Kaltenbach, M. A. Horner, J. H. Rothman, S. E. Mango, *Mol. Cell* **6**, 705 (2000).
9. J. C. Dantonel, S. Quintin, L. Lakatos, M. Labouesse, L. Tora, *Mol. Cell* **6**, 715 (2000).
10. G. J. C. Veenstra, D. L. Weeks, A. P. Wolffe, *Science* **290**, 2312 (2000).
11. Supplementary information is available on *Science* Online (www.sciencemag.org/cgi/content/full/1059188/DC1).
12. A. R. Bellve *et al.*, *J. Cell Biol.* **74**, 68 (1977).
13. F. Nantel *et al.*, *Nature* **380**, 159 (1996).
14. D. Zhang, in preparation.
15. S. Kashiwabara, Y. Arai, K. Kodaira, T. Baba, *Biochem. Biophys. Res. Commun.* **173**, 240 (1990).
16. Z. F. Zakeri, D. J. Wolgemuth, C. R. Hunt, *Mol. Cell. Biol.* **8**, 2925 (1988).
17. B. Drabent, C. Bode, B. Bramlage, D. Doenecke, *Histochem. Cell Biol.* **106**, 247 (1996).
18. M. Matsumoto, H. Fujimoto, *Biochem. Biophys. Res. Commun.* **166**, 43 (1990).
19. K. C. Kleene *et al.*, *Dev. Biol.* **137**, 395 (1990).
20. J. E. Welch, E. C. Schatte, D. A. O'Brien, E. M. Eddy, *Biol. Reprod.* **46**, 869 (1992).
21. K. D. Fulcher *et al.*, *Biol. Reprod.* **52**, 41 (1995).
22. D. Wouters-Tyrou, A. Martinage, P. Chevaillier, P. Sautiere, *Biochimie* **80**, 117 (1998).
23. Y. E. Yu *et al.*, *Proc. Natl. Acad. Sci. U.S.A.* **97**, 4683 (2000).
24. E. M. Eddy, *Semin. Cell Dev. Biol.* **9**, 451 (1998).
25. J. A. Blendy, K. H. Kaestner, G. F. Weinbauer, E. Nieschlag, G. Schutz, *Nature* **380**, 162 (1996).
26. R. Behr, N. Hunt, R. Ivell, J. Wessels, G. F. Weinbauer, *Biol. Reprod.* **62**, 1344 (2000).
27. G. M. Fimia, D. De Cesare, P. Sassone-Corsi, *Mol. Cell. Biol.* **20**, 8613 (2000).
28. ———, *Nature* **398**, 165 (1999).
29. T. Diemer, C. Desjardins, *Hum. Reprod. Update* **5**, 120 (1999).

30. We are grateful to the Laboratory of Animal Research Center of the Rockefeller University for mouse work. We also thank M. Hardy, M. Ito, and U. Kim for technical help and for critical discussion of the manuscript. This work was supported by NIH grants to R.G.R and P.L.M and by postdoctoral fellowships from the Norman Winston Foundation to D.Z. and from Deutsche Forschungsgemeinschaft Leukemia Research Foundation to M.T.

19 January 2001; accepted 3 April 2001
Published online 12 April 2001;
10.1126/science.1059188
Include this information when citing this paper.

The Foot-and-Mouth Epidemic in Great Britain: Pattern of Spread and Impact of Interventions

Neil M. Ferguson,* Christl A. Donnelly, Roy M. Anderson

We present an analysis of the current foot-and-mouth disease epidemic in Great Britain over the first 2 months of the spread of the virus. The net transmission potential of the pathogen and the increasing impact of control measures are estimated over the course of the epidemic to date. These results are used to parameterize a mathematical model of disease transmission that captures the differing spatial contact patterns between farms before and after the imposition of movement restrictions. The model is used to make predictions of future incidence and to simulate the impact of additional control strategies. Hastening the slaughter of animals with suspected infection is predicted to slow the epidemic, but more drastic action, such as "ring" culling or vaccination around infection foci, is necessary for more rapid control. Culling is predicted to be more effective than vaccination.

A new epidemic of foot-and-mouth disease (FMD) (also known as hoof-and-mouth disease) began in Great Britain in February 2001, 34 years since the last major outbreak. From the primary infection of a pig herd in Northumberland in early February, the disease spread rapidly via long-distance animal movements and also spread locally via contact and windborne transmission (*1*). The initial spread was greatly influenced by the fre-